JACS
JOURNAL OF THE AMERICAN CHEMICAL SOCIETY

ARTICLE

pubs.acs.org/JACS

Structure of Peptides on Metal Oxide Surfaces Probed by NMR

Peter A. Mirau,* Rajesh R. Naik, and Patricia Gehring

Materials and Manufacturing Directorate, Nanostructured and Biological Materials Branch, Air Force Research Laboratories, Wright-Patterson AFB, Ohio 45433, United States

Supporting Information

ABSTRACT: Peptides that bind inorganic surfaces and template the formation of nanometer-sized inorganic particles are of great interest for the self- or directed assembly of nanomaterials for sensors and diagnostic applications. These surface-recognizing peptides can be identified from combinatorial phage-display peptide libraries, but little experimental information is available for understanding the relationship between the peptide sequence, structure at the nanoparticle surface, and function. We have developed NMR methods to determine the structures of peptides bound to inorganic nanoparticles and report on the structure of three peptides bound to silica and titania surfaces. Samples were prepared under conditions leading to rapid peptide exchange at the surface such that solution-based nuclear Overhauser experiments can be used to determine the three-dimensional structure of the bound peptide. The binding motif is defined by a compact "C"-shaped structure for the first six amino acids in the 12-mer. The orientation of the peptide on the nanoparticle surface was determined by magnetization transfer from the nanoparticle surface to the nearby peptide protons. These methods can be applied to a wide variety of abiotic interfaces to provide an insight into the relationship between the primary sequence of peptides and their functionality at the interface.

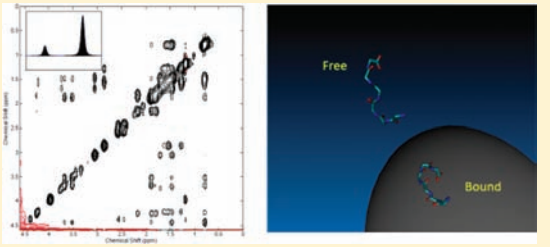

INTRODUCTION

Nanomaterials are of great interest for sensors and other electronic devices because of their size-dependent optical, electrical, and magnetic properties.[1,2] Functionality in nanoparticle-based sensors often depends not only on the nanoparticle properties, but also on the interactions between nanoparticles, which may be altered by the binding of a target substance.[3−5] Surface modification is also important for the self-assembly and/or dispersion of nanoparticles in a host matrix.[6]

The two greatest challenges in designing sensors for chemical and biological applications are sensitivity and selectivity. One promising approach is to use biological molecules as recognition elements,[7] because it is well-known from enzyme and antibody studies that biomolecules are able to differentiate between subtle differences in chemical structure. Biological organisms are also extremely efficient at detecting and responding to low concentrations of biomarkers, including signaling peptides and hormones. One strategy for designing peptides as recognition elements in sensors uses fusion peptides constructed from combinations of functional peptides. Recent examples of this approach include the use of a fusion peptide that recognizes both carbon nanotubes and TNT as the functional element in a field-effect transistor,[8] and bimetallic fusion peptides that function as metal ion sensors.[9]

A number of peptides that recognize inorganic surfaces have been identified from natural sources[10,11] and combinatorial peptide phage-display libraries.[12−14] The phage-display experiments start with a large number of random peptide sequences (10^9) and typically identify a few sequences that strongly bind to the target material. When tested by quartz-crystal microbalances or surface-plasmon resonance, the isolated peptide sequences (12-mers or 7-mers) often show strong ($K_d = \mu M$) binding to the targeted surfaces.[15,16] In addition, the surface-binding peptides are often effective at templating the formation of nanometer-sized, monodisperse metal or metal oxide particles.[17]

The grand challenge for understanding how peptides interact with inorganic surfaces is determining the relationship between the peptide primary sequence and the functionality (binding or templating). To date, sequence comparisons of surface-binding peptides have not provided a fundamental understanding of how peptides interact with inorganic surfaces, and relatively little is known about the structure of peptides at surfaces because these systems are difficult to study experimentally. Early NMR studies showed that poly-L-lysine and poly-L-glutamic acid undergo a transition from an α-helical to a more extended conformation upon silica and hydroxapatite binding,[18] and statherin is disordered in solution but adopts an α-helical conformation TFE/water solutions[19] and at the hydroxyapatite surface.[10] Circular dichroism studies generally show a change in the peptide conformation upon binding to inorganic surfaces,[15,20,21] but it is difficult to relate these changes directly to the molecular structure. Molecular dynamics simulations and coarse grain molecular modeling has been applied to peptides binding to both metal[15,22,23] and metal oxide surfaces,[24−26] but in general the results do not show specific conformations bound to the

Received: June 13, 2011
Published: October 07, 2011

surface. It is generally observed that phage-selected peptides exhibit a random-coil conformation in the absence of the target substance.[27,28]

One means to understand structure/function relationships is to determine the three-dimensional structure of peptides bound to inorganic surfaces so that the interactions that drive recognition and stabilize binding can be identified. Solid-state NMR with site-specific isotopic labeling has been used to determine the structure of statherin, a 43-amino acid peptide, bound to the surface of hydroxyapaptite.[10] The α-helical structure of statherin was determined by measuring the dipolar couplings between ^{13}C and ^{15}N labels in nearby amino acids, and the peptide orientation on the surface was deduced from dipolar couplings between the peptide and the surface atoms. This methodology is in principle applicable to a wide variety of peptide recognition problems but requires isotopically labeled peptides.

The peptide of interest in our studies is the 12-mer titania binding peptide (TBP12, RKLPDAPGMHTW) identified from phage-display experiments as a strong binder to TiO_2 (K_d = 13.2 μM), SiO_2 (K_d = 11.1 μM) and silver but not other metals (Au, Cr, Pt, Sn, Zn, Cu, or Fe).[16,29] Alanine substitution experiments showed that the first six amino acids are most important for surface recognition, and that alanine substitution at Lys2 increased the binding strength while substitution at Arg1, Pro4, or Asp5 leads to weaker binding.

In these studies we have used high-resolution solution NMR methods, including nuclear Overhauser effect spectroscopy (NOESY)[30] and saturation-transfer difference (STD)[31] NMR, to determine the structure and orientation of peptides bound to SiO_2 and TiO_2 nanoparticle surfaces. We obtained high-resolution spectra by choosing conditions under which the peptide is rapidly exchanging with the nanoparticle surface. The NOESY cross-peaks arise predominantly from the bound conformation, so the structure can be determined using the standard methods for NMR protein structure determination.[30] In addition we show how magnetization transfer from the nanoparticle surface can be used to determine the binding orientation. With the development of these methods we are now in the position to determine the relationship between the primary sequence of peptides and their abilities to recognize and bind surfaces.

EXPERIMENTAL SECTION

Buffer reagents and deuterated water were obtained from Aldrich. Peptides were purchased from New England Peptide with a purity greater than 95% as shown by HPLC. Silica nanoparticles were obtained by sonicating fumed silica (Aldrich) with a nominal particle size of 14 nm and a surface area of 200 m^2/g. The 25 nm TiO_2 particles were obtained from DeGussa.

All experiments were performed in 0.02 M phosphate buffer at pH 7. Nanoparticle mixtures were prepared by dissolving the appropriate amount of nanoparticle in water followed by horn sonication for 5 min at a 33% duty cycle. The nanoparticles were mixed with buffered peptide solutions (1 mg/mL) in 90:10 H_2O:D_2O or D_2O.

NMR experiments were performed on a Bruker Avance 400 MHz NMR spectrometer at 298 K using the standard 2D NOESY, TOCSY, and ROESY pulse sequences[32] with WATERGATE[33] for solvent suppression. Distance constraints from the NOESY spectra were used as input for the XPLOR[34] program to determine the three-dimensional structure. The structures were refined against the experimental NOESY data using in-house Matlab programs and visualized with VMD.[35]

The orientation of the peptide on the surface was measured by saturation-transfer difference NMR[31] using low-powered Gausian-shaped pulses to achieve saturation and WATERGATE[33] for signal detection. Difference spectra were taken between experiments with the saturation pulses (2 s) centered at −2 and 30 ppm.

Table 1. Peptide Sequences and Nomenclature

peptide	sequence
TBP6	RKLPDA
A2TBP6	RALPDA
TBP12	RKLPDAPGMHTW
A2TBP12	RALPDAPGMHTW

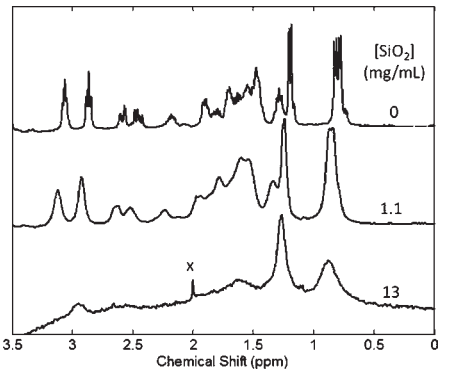

Figure 1. The effect of 14 nm silica nanoparticles on the proton NMR spectrum of the peptide TBP6. Impurities from the nanoparticle are marked (x).

RESULTS AND DISCUSSION

We have used solution NMR to determine the structure of peptides bound to inorganic surfaces by preparing peptide/nanoparticle solutions in which the peptide is rapidly exchanging with the inorganic surface. The peptides of interest (Table 1) are deletions and mutants of the TBP12 peptide that strongly binds silica and titania surfaces.[16,29]

Figure 1 shows the NMR spectra of TBP6 as the concentration of silica nanoparticles (14 nm) is increased from 0 to 13 mg/mL. In the absence of nanoparticles, sharp lines are observed for the peptide, as expected for such a low molecular weight (701 g/mol) material. The lines slightly broaden and shift as the nanoparticle concentration is increased to 1 mg/mL and are greatly broadened at higher (13 mg/mL) nanoparticle concentrations. Such behavior is commonly observed for molecules exchanging between two magnetically distinct environments. The line broadening is a consequence of the change in proton chemical shift for the peptide upon binding to the nanoparticle and depends on exchange rate and the populations of free and bound peptide.[36] At high nanoparticle concentrations, the peptide is completely bound and the line width is determined by the rate of reorientation of the nanoparticles. Similar changes in the chemical shifts and line widths are observed in the presence of 25 nm titania and 7 nm silica nanoparticles (Figure S1, Supporting Information). While the spectra show some dependence on the size and source of the nanoparticles, it is possible to choose the temperature, ionic strength, nanoparticle concentration, or peptide concentration such that the peptide is in fast exchange with the nanoparticle surface.

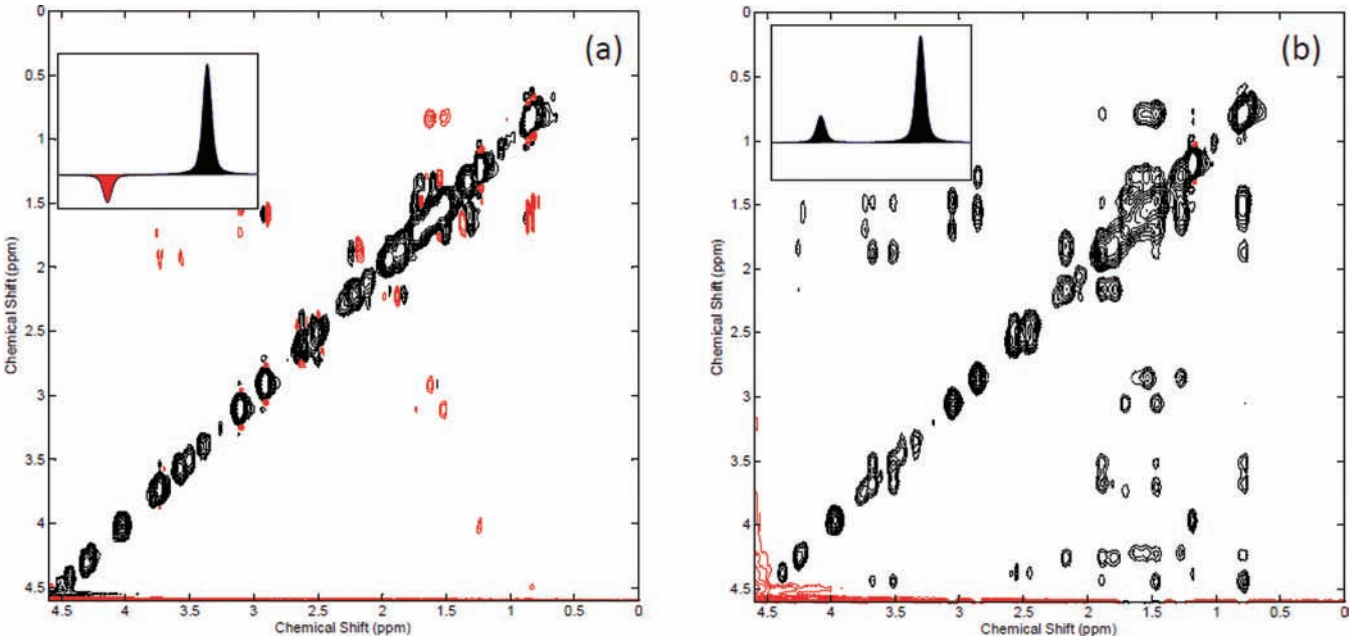

Figure 2. The 2D NOESY spectra of RKLPDA in the (a) absence and (b) presence of 1 mg/mL titania 25 nm nanoparticles. The inset plots show the relative signs of the diagonal and cross-peaks expected in the (a) fast and (b) slow motion limit.

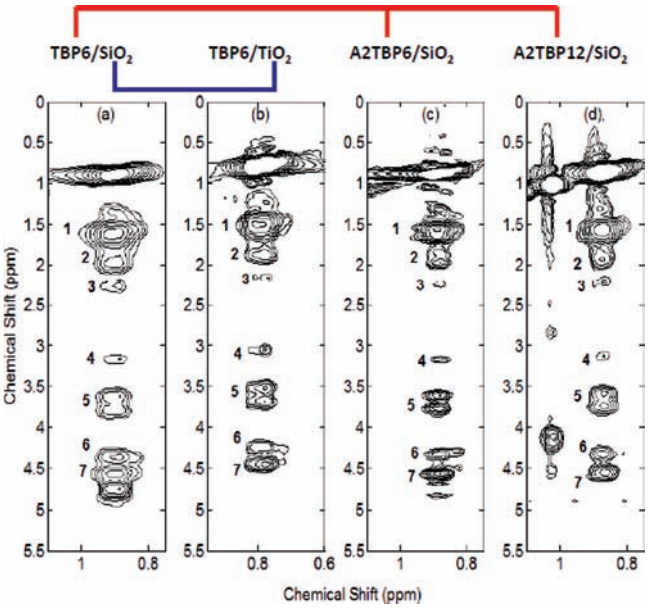

Figure 3. Comparison of the 2D NOESY spectra for peptides bound to silica and titania. The plots show the Leu3 Hδ cross-peaks for (a) the RKLPDA/SiO_2, (b) RKLPDA/TiO_2, (c) RALPDA/SiO_2, and (d) RALPDAPGMHTW/SiO_2 complexes. The peak labels denote the cross-peaks between the Leu3 Hδ methyl protons and (1) Leu3 Hγ, (2) Pro4 Hγ, (3) Pro4 Hβ, (4) Arg1 Hδ, (5) Pro4 Hδ, (6) Pro4 Hα, and (7) Leu3 Hα.

Nuclear Overhauser effects (NOEs) are extremely useful for protein structure determination because the cross-peak intensities depend on the inverse sixth power of the internuclear distances.[30] The NOEs can be used to identify the peptides bound to the nanoparticle surface because the sign and magnitude of the NOE depends on the rate of reorientation in solution. Low molecular weight peptides have weakly positive NOEs while the NOEs for peptides bound to a nanometer-sized particles are much stronger and negative. We can distinguish between the free and bound peptide by observing the sign of the NOE cross-peaks relative to the diagonal peaks in the 2D NOESY experiment.[37]

Figure 2 compares the 2D NOESY spectrum of TBP6 in the presence and absence of 25 nm titania nanoparticles (1 mg/mL). The peaks are color coded (positive/negative) to show the sign of the cross-peaks relative to the diagonal. The cross-peaks for TBP6 in the absence of nanoparticles are opposite in sign from the diagonal, as expected for a low molecular weight peptide. In contrast, the cross-peaks have the same sign as the diagonal in the presence of nanoparticles, indicating that the dynamics are in the slow motion regime. Such behavior is expected for peptides that are rapidly exchanging on and off the surface of the slowly tumbling nanoparticles. Negative NOEs are observed because magnetization exchange is much more efficient on the surface of the nanoparticles compared to the free peptide.

The NOEs observed for the bound peptides can be used not only to determine the three-dimensional structure of the peptide bound at the inorganic surface but also to identify the amino acids that contribute to surface recognition. Figure 3 compares sections of the 2D NOESY spectra showing interactions of the Leu3 Hδ methyl protons with nearby protons for the TBP6/SiO_2, TBP6/TiO_2, A2TBP6/SiO_2, and A2TBP12/SiO_2 complexes. The feature to note in Figure 3 is that similar cross-peak patterns are observed for the TBP6 bound to either silica (TBP6/SiO_2) or titania (TBP6/TiO_2), the hexamer with alanine at the second position bound to silica (A2TBP6/SiO_2), and the alanine-substituted dodecamer bound to silica (A2TBP12/SiO_2). These raw data strongly suggest that that the peptides adopt similar conformations at the surface of silica and titania, and that the bound conformation does not depend on the presence of the charged lysine at the second position.

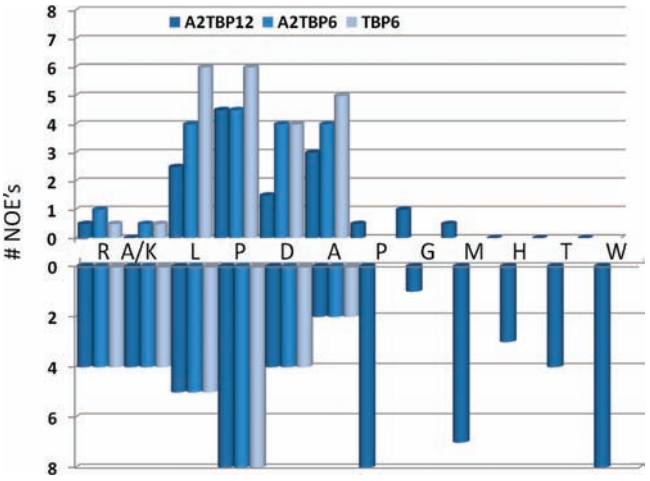

Figure 4. The number of (bottom) intraresidue and (top) inter-residue NOEs observed for RKLPDA, RALPDA, and RALPDAPGMHTW bound to silica nanoparticles. All NOEs are negative.

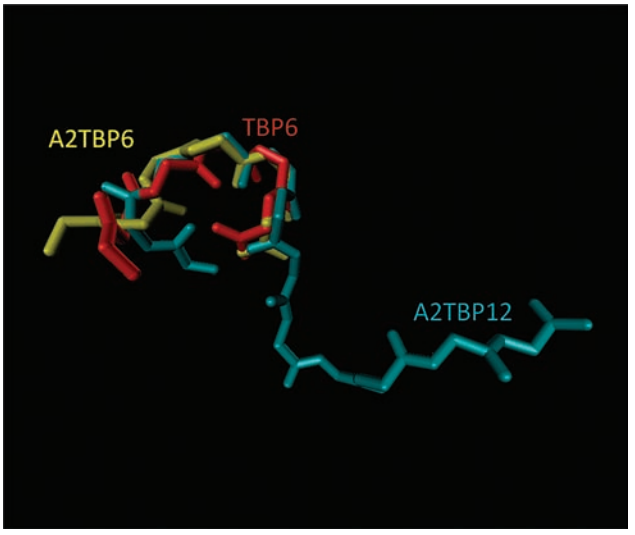

Figure 5. Overlay of the refined structures of the A2TBP6, TBP6, and A2TBP12 bound to the surface of silica nanoparticles. Only backbone atoms are shown.

The medium and long-range NOEs critical for protein structure determination are not observed in the short peptides studied here, so the structure must be determined from the pattern of intra- and inter-residue NOEs. The intraresidue NOEs are often not useful for structure determination because the distances are constrained by the chemical bonds. One important exception is the NH−Hα distance that depends on the Φ torsional angle in the peptide backbone.[30]

The general features of the bound peptides can be determined from Figure 4, which shows a plot of the number of intra- and inter-residue NOEs observed for TBP6, A2TBP6 and A2TBP12 bound to silica nanoparticles. The data shows that the majority of inter-residue NOEs are observed for the Leu3-Ala6 portion of the sequence. Furthermore, we do not observe a large increase in the number of inter-residue cross-peaks in the dodecamer complex (A2TBP12/SiO_2) complex relative to the hexamer (A2TBP6/SiO_2) complex. With the exception of some

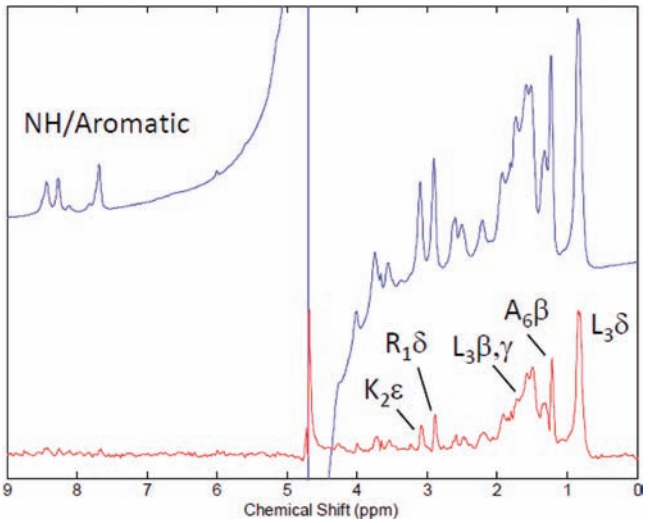

Figure 6. Comparison of the off-resonance control spectrum (top) and the saturation-transfer difference spectrum for the TBP6/SiO_2 complex. The saturation-transfer difference spectrum is increased by a factor of 10 relative to the control.

intraresidue cross-peaks (Trp12 H2−Hβ and His10 H2−Hβ), no significant cross-peaks are observed to the aromatic protons of Trp12 and His10. Inter-residue cross-peaks are observed, however, between Gly8 Hα-Met9 NH and Thr11 NH-Trp12 Hβ. Taken together, these data confirm that only the first six amino acids are critical for surface recognition.

The structures of the peptides bound to inorganic surfaces were determined using the NOEs as input for the XPLOR structure determination program[34] and refined using Matlab programs to simulate the 2D spectra from the coordinates of the refined structures. The output from XPLOR is a family of structures that satisfy the distance constraints. As anticipated from the pattern of NOEs shown in Figure 4, only the first six amino acids of A2TBP12 have a sufficient number of NOEs to constrain the structure. This is illustrated in the overlay of the family of acceptable structures for A2TBP12 bound to silica (Figure S2, Supporting Information) in which the first six amino acids can be aligned, but no common structure is observed for the remaining six amino acids. This result is consistent with the alanine substitution experiments[16] and might be expected because the peptides do not have free N-terminal and C-terminal ends in the phage-display selection experiments. The displayed peptides in the phages may not have the conformational flexibility to allow all amino acids to simultaneously interact with the target material.

Figure 5 shows an overlay of typical accepted structures for TBP6, A2TBP6, and A2TBP12 bound to silica nanoparticles, where the structures have been aligned using the backbone atoms of residues 2−5. The important feature to note is that similar structures are observed for all three peptides bound to the silica surface. The hexamer structure is not extended but partially folded into a "C" shape to accommodate the NOEs observed in all structures between the Arg1 Hδ and the Leu3 Hδ. Although it is not possible to exclude contributions from low concentrations of alternate conformations, the peaks in the 2D spectra are well represented by these structures, suggesting that the bound conformation closely resembles the structures shown in Figure 5. Given the relatively small number of restraints for the peptide at

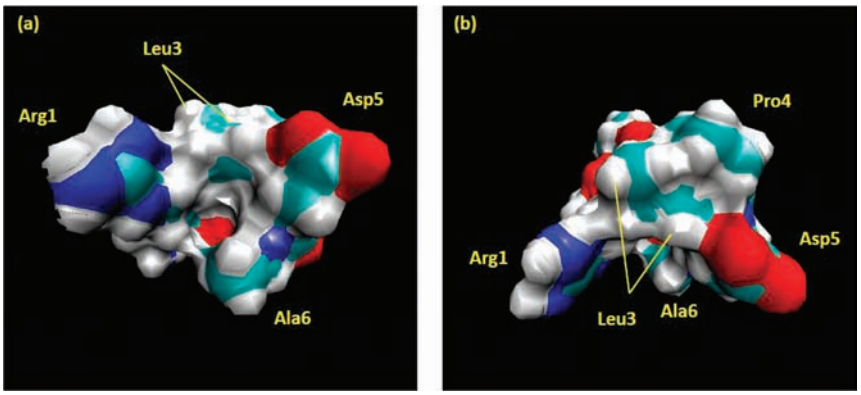

Figure 7. Surface representations of the TBP6 peptide at the nanoparticle surface. The illustrations show how the face of the peptide interacting with the surface places the leucine and alanine methyl protons in close contact with the surface. Drawing b is rotated 90° from drawing a.

the surface, the resolution of the structure of the surface-bound peptide is not as high as that reported for proteins with many more constraints per amino acid.

The experiments presented thus far show the structure of the bound peptides, but provide no insight into the interactions between the peptides and the inorganic surfaces. We have explored this interaction using saturation-transfer difference (STD) NMR,[31] an experiment that has been extensively used to measure fast-exchange ligand binding to proteins. STD experiments take advantage of the difference in line widths for the peptide and the nanoparticle. The slowly tumbling nanoparticle has tightly bound water and hydroxyl protons that give rise to broad (and unobservable) lines. We can irradiate the edge of this line in a part of the spectrum (−2 ppm) that does not overlap with the free peptide and can saturate the water/hydroxyl groups at the nanoparticle surface. Because the nanoparticles are tumbling slowly, there is rapid magnetization exchange among the surface protons. This magnetization can be transferred to the peptide when it binds on the surface, and peaks in close proximity to the surface can be identified from the difference spectra.

Figure 6 shows the STD NMR spectra for TBP6 bound to the surface of silica nanoparticles. A number of signals are observed in the difference spectra, including those from the Ala6, Leu3, Lys2, and Arg1 side-chain protons. It is interesting to note that difference peaks are only observed for the side-chain protons and not the main-chain amide protons in the 7.5−8.5 ppm range. The STD spectra for the A2TBP12/SiO_2 complex (Figure S3, Supporting Information) also show surface side-chain interactions but no peaks for the aromatic or NH signals.

It was somewhat surprising that peaks from the more hydrophobic leucine and alanine side chains appear in the STD spectra because we expect the surface of silica nanoparticles to be hydrophilic. This observation can be explained by considering the surface representations of the TBP6 peptide bound to the silica surface shown in Figure 7. The peptide forms a compact "C"-shaped structure on the nanoparticle surface with the Leu3 and Ala6 methyl groups displayed on one face. We believe that it is this face of the peptide that directly contacts the metal oxide surface. It is not possible to determine if interactions of the leucine methyl groups contribute to the free energy of binding, or if they are placed in close proximity as a consequence of the interactions of the polar groups (carbonyl, amino, carboxylic acid) with the hydrophilic surface. We also note the presence of the STD peaks from charged side-chain residues (Arg1 Hδ and Lys2 Hε) in Figure 6. These data suggest that ionic interactions between the ends of these amino acid side chains and the surface help to anchor the peptide. Studies with ^{13}C- and ^{15}N-labeled peptides would allow us to study the structure and dynamics of the N-terminal and C-terminal segments in greater detail.

CONCLUSION

We have used NMR to determine the structure of three related peptides bound to silica and titania nanoparticles by taking advantage of the peptide exchange kinetics and using solution NMR methods. The peptide structures are similar for three sequence variants binding to silica and titania, suggesting a common binding motif. The combination of NMR refinement and STD NMR allows us to determine both the conformation and the orientation of the peptide on the nanoparticle surface. Our goal is to determine the structure of a large number of peptides bound to inorganic surfaces so that we can understand the relationship between the primary sequence of peptides and their ability to recognize inorganic surfaces.

ASSOCIATED CONTENT

Supporting Information. Additional experimental procedures and supplementary figures. This material is available free of charge via the Internet at http://pubs.acs.org.

AUTHOR INFORMATION

Corresponding Author
peter.mirau@wpafb.af.mil

REFERENCES

(1) Cao, G.; Wang, Y. *Nanostructures and Nanomaterials: Synthesis, Properties, and Applications*; World Scientific Publishing Co., Inc.: Hackensack, NJ, 2011.
(2) *Carbon Nanotubes: Synthesis, Structure, Properties and Applications*; Smalley, R. E.; Dresselhaus, M. S.; Dresselhaus, G.; Avouris, P., Eds.; Springer: New York, 2001.
(3) Aragay, G.; Pons, J.; Merkoçi, A. *Chem. Rev.* **2011**, *111*, 3433.
(4) Liu, J.; Cao, Z.; Lu, Y. *Chem. Rev.* **2009**, *109*, 1948.
(5) Talapin, D. V.; Lee, J.-S.; Kovalenko, M. V.; Shevchenko, E. V. *Chem. Rev.* **2009**, *110*, 389.
(6) Vaia, R. A.; Maguire, J. F. *Chem. Mater.* **2007**, *19*, 2936.
(7) McConney, M. E.; Anderson, K. D.; Brott, L. L.; Naik, R. R.; Tsukruk, V. V. *Adv. Funct. Mater.* **2009**, *19*, 2527.

(8) Kuang, Z. F.; Kim, S. N.; Crookes-Goodson, W. J.; Farmer, B. L.; Naik, R. R. *ACS Nano* **2010**, *4*, 452.
(9) Slocik, J. M.; Zabinski, J. S., Jr.; Phillips, D. M.; Naik Rajesh, R. *Small* **2008**, 548.
(10) Goobes, G.; Stayton, P. S.; Drobny, G. P. *Prog. Nucl. Magn. Reson. Spectrosc.* **2007**, *50*, 71.
(11) Kroger, N.; Deutzmann, R.; Sumper, M. *Science* **1999**, *286*, 1129.
(12) Brown, S. *Nat. Biotechnol.* **1997**, *15*, 269.
(13) Naik, R. R.; Brott, L. L.; Clarson, S. J.; Stone, M. O. *J. Nanosci. Nanotechnol.* **2002**, *2*, 95.
(14) Whaley, S. R.; English, D. S.; Hu, E. L.; Barbara, P. F.; Belcher, A. M. *Nature* **2000**, *405*, 665.
(15) Hnilova, M.; Oren, E. E.; Seker, U. O. S.; Wilson, B. R.; Collino, S.; Evans, J. S.; Tamerler, C.; Sarikaya, M. *Langmuir* **2008**, *24*, 12440.
(16) Sano, K. I.; Sasaki, H.; Shiba, K. *Langmuir* **2005**, *21*, 3090.
(17) Dickerson, M. B.; Sandhage, K. H.; Naik, R. R. *Chem. Rev.* **2008**, *108*, 4935.
(18) Fernandez, V. L.; Reimer, J. A.; Denn, M. M. *J. Am. Chem. Soc.* **1992**, *114*, 9634.
(19) Gururaja, T. L.; Naganagowda, G. A.; Levine, M. J. *J. Biomol. Struct. Dynam.* **1998**, *16*, 91.
(20) Coppage, R.; Slocik, J. M.; Sethi, M.; Pacardo, D. B.; Naik, R. R.; Knecht, M. R. *Angew. Chem., Int. Ed.* **2010**, *122*, 3855.
(21) Slocik, J. M.; Govorov, A. O.; Naik, R. R. *Nano Lett.* **2011**, *11*, 701.
(22) Pandey, R. B.; Heinz, H.; Feng, J.; Farmer, B. L.; Slocik, J. M.; Drummy, L. F.; Naik, R. R. *Phys. Chem. Chem. Phys.* **2009**, *11*, 1989.
(23) Heinz, H.; Farmer, B. L.; Pandey, R. B.; Slocik, J. M.; Patnaik, S. S.; Pachter, R.; Naik, R. R. *J. Am. Chem. Soc.* **2009**, *131*, 9704.
(24) Lenoci, L.; Camp, P. J. *J. Am. Chem. Soc.* **2006**, *128*, 10111.
(25) Patwardhan, S. V.; Patwardhan, G.; Perry, C. C. *J. Mater. Chem.* **2007**, *17*, 2875.
(26) Skelton, A. A.; Liang, T.; Walsh, T. R. *ACS Appl. Mater. Interfaces* **2009**, *1*, 1482.
(27) Kulp, J. L.; Sarikaya, M.; Evans, J. S. *J. Mater. Chem.* **2004**, *14*, 2325.
(28) Kulp, J. L.; Shiba, K.; Evans, J. S. *Langmuir* **2005**, *21*, 11907.
(29) Sano, K. I.; Shiba, K. *J. Am. Chem. Soc.* **2003**, *125*, 14234.
(30) Wuthrich, K. *NMR of Proteins and Nucleic Acids*; John Wiley & Sons: New York, 1986.
(31) Mayer, M.; Mayer, B. *J. Am. Chem. Soc.* **2001**, 123.
(32) *Two-Dimensional NMR. Applications for Chemists and Biochemists*; Croasmun, W. R.; Carlson, M. K., Eds.; VCH Publishers, Inc.: New York, 1994.
(33) Piotto, M.; Saudek, V.; Sklenar, V. *J. Biomol. NMR* **1992**, *2*, 661.
(34) Schwietters, C. D.; Kuszewski, J. J.; Clore, G. *Prog. Nucl. Magn. Reson. Spectrosc.* **2006**, *48*, 47.
(35) Humphrey, W.; Dalke, A.; Schulten, K. *J. Mol. Graphics* **1996**, *14*, 33.
(36) Abragam, A. *Principles of Nuclear Magnetism*; Oxford University Press: New York, 1961.
(37) Neuhaus, D.; Williamson, M. *The Nuclear Overhauser Effect in Structural and Conformational Analysis*; VCH Publishers Inc.: New York, 1989.